

The Reaction Mechanism and Kinetics Data of Racemic Atenolol Kinetic Resolution via Enzymatic Transesterification Process Using Free *Pseudomonas fluorescens* Lipase

JONI AGUSTIAN,¹ AZLINA HARUN KAMARUDDIN²

¹Department of Chemical Engineering, Universitas Lampung, Bandar Lampung, 35145, Lampung, Indonesia

²School of Chemical Engineering, Universiti Sains Malaysia, 14300 Nibong Tebal, Seberang Perai Selatan, Penang, Malaysia

Received 18 August 2015; revised 16 December 2015; accepted 8 February 2016

DOI 10.1002/kin.20986

Published online 15 March 2016 in Wiley Online Library (wileyonlinelibrary.com).

ABSTRACT: A thorough study on free-enzyme transesterification kinetic resolution of racemic atenolol in a batch system was investigated to gain knowledge for (S)-atenolol kinetics. Analyses of enzyme kinetics using Sigma-Plot 11 Enzyme Kinetics Module on the process are based on Michaelis–Menten and Lineweaver–Burk plot, which give first-order reaction and ordered-sequential Bi–Bi mechanism, where V_{\max} , K_M -vinyl acetate, and K_M -(S)-atenolol are 0.80 mM/h, 29.22 mM, and 25.42 mM, respectively. Further analyses on enzyme inhibitions find that both substrates inhibit the process where (S)-atenolol and vinyl acetate develop competitive inhibition and mixed inhibition, respectively. Association of (S)-atenolol with free enzyme to inhibit the enzyme is higher than reaction of active enzyme–substrate complex with vinyl acetate. © 2016 Wiley Periodicals, Inc. *Int J Chem Kinet* 48: 253–265, 2016

INTRODUCTION

Atenolol chemically known as 2-{4-[2-hydroxy-3-(propan-2-ylamino)propoxy]phenyl} acetamide is a

Correspondence to: Azlina Harun Kamaruddin; e-mail: chazlina@usm.my.

© 2016 Wiley Periodicals, Inc.

β 1-selective β -adrenergic receptor blocking drug used to treat chest pain, hypertension, and heart attack. The drug is recognized as one of the best-selling drugs in the world [1–3]. It is mainly sold in the form of racemic mixture. This β -blocker depends on its β -blocking activity on (*S*)-enantiomer. The eudismic ratio of the compound is 46 [4]. Because (*R*)-atenolol has no β -blocking activity and brings side effects [5,6], switching from the racemic atenolol to (*S*)-atenolol produces lesser side effects [7].

Two ways are developed to make the (*S*)-atenolol: asymmetric synthesis and resolution of the available racemic atenolol. The asymmetric synthesis via the chemo-catalysis process required chiral chemical catalysts such as bimetallic chiral [Co(salen)]-type complexes to be used to convert racemic or achiral substrates hydrolytically or directly [8–11]. The compound was also synthesized asymmetrically via the chemo-enzymatic catalysis process of 4-hydroxyphenylacetamide and chiral epichlorohydrin using NaOH and immobilized *Candida antarctica* lipase A (CAL-A CLEA) as the catalysts, which was claimed as the greener process over other methods [12]. It was made by reacting achiral feeds with the availability of chiral addenda as well [13–15]. Although the asymmetric syntheses provide outstanding choices, they frequently use low reaction temperature and long reaction steps. Besides, the chiral catalysts are still expensive.

The second way uses the existing racemic atenolol as the substrate for the (*S*)-atenolol formation. The racemate was resolved via microbial (whole-cells) fermentation, which gave high yield and enantiomeric excess [16], enzymatic kinetic resolution using immobilized lipases [17,18], or liquid chromatography process using specific chiral selectors [19,20]. The fermentation process should consider preparation and recovery of the whole cells when this technology is applied. The liquid chromatography frequently needs tedious sample preparations, expensive chiral columns, and large volumes of additives [21]. The kinetic resolution process using immobilized enzymes utilized diatomite earth and Eupergit–Carbon as the enzyme support. These immobilized enzymes need a sort of enzyme recycle system to reuse the enzyme in the process.

Nowadays, enzymes can be immobilized onto the membrane surfaces to form enzymatic membrane reactors (EMR) that can operate continuously and be used repeatedly. They could give a better prospect on the racemic atenolol resolution. Proper enzyme(s) must first be chosen as the EMR require free enzyme(s) to be attached onto the surfaces. Hence, screening of free enzymes must be conducted before the EMR process

is made available. However, no report on free enzyme-based racemic atenolol kinetic resolution was found. Therefore, we studied the kinetic resolution of racemic atenolol via enzymatic transesterification using free *Pseudomonas fluorescense* lipase (Amano) and vinyl acetate in tetrahydrofurane to gain knowledge for the (*S*)-atenolol preparation. Herewith, the kinetics study of the resolution process is reported since determination of the kinetics data is important for better understanding and scaleup of the resolution process [22].

EXPERIMENTAL

Materials

The (*R,S*)-atenolol (99% USP) purchased from Nanjing Chemlin Chemical Industry (Nanjing, People's Republic of China) was used. The calibration curves were prepared from the (*S*)-atenolol (97%; Tocris Bioscience, Bristol, UK) and (*R*)-atenolol (99%; Sigma Aldrich, Selangor, Malaysia). The chemicals were of analytical grade except for analysis (of HPLC grade) supplied by EOS Scientific (Selangor, Malaysia), Fisher Scientific (Selangor, Malaysia), and Merck (Selangor, Malaysia). *Pseudomonas fluorescense* lipase (Amano, product no. 534730, 20 U/mg) was bought from Modern-Lab Chemicals (Penang, Malaysia). The racemate, single enantiomers, lipase, and all chemicals were used without pretreatment.

Procedure and Analysis

The racemic atenolol and vinyl acetate concentration were set in the range of 3.75–30.04 and 43.4–86.8 mM, respectively. Both concentrations were acquired from the previous experiments (the data are not shown). The concentration of the racemate was kept constant when vinyl acetate quantities were varied and vice versa. Fifty milliliters of 18.80 mM racemic atenolol dissolved in tetrahydrofurane was prepared in some 100 mL flasks. Then vinyl acetate at different quantities was mixed into each flask. After the flasks were shaken for 30 min, every flask was added with enzyme. All experiments used operating conditions obtained from the optimization step (45°C, 190 rpm, 2000 U *Pseudomonas fluorescense* lipase (PFL)). The mixtures were incubated in orbital shakers (Max Q4000 Barnstead Lab-Lin). Samples were taken on certain time interval and were analyzed chromatographically. The data were processed using Sigma-Plot 11 Enzyme Kinetics Module.

Atenolol enantiomers were observed using Chiralcel® OD column (250 mm × 4.6 mm)

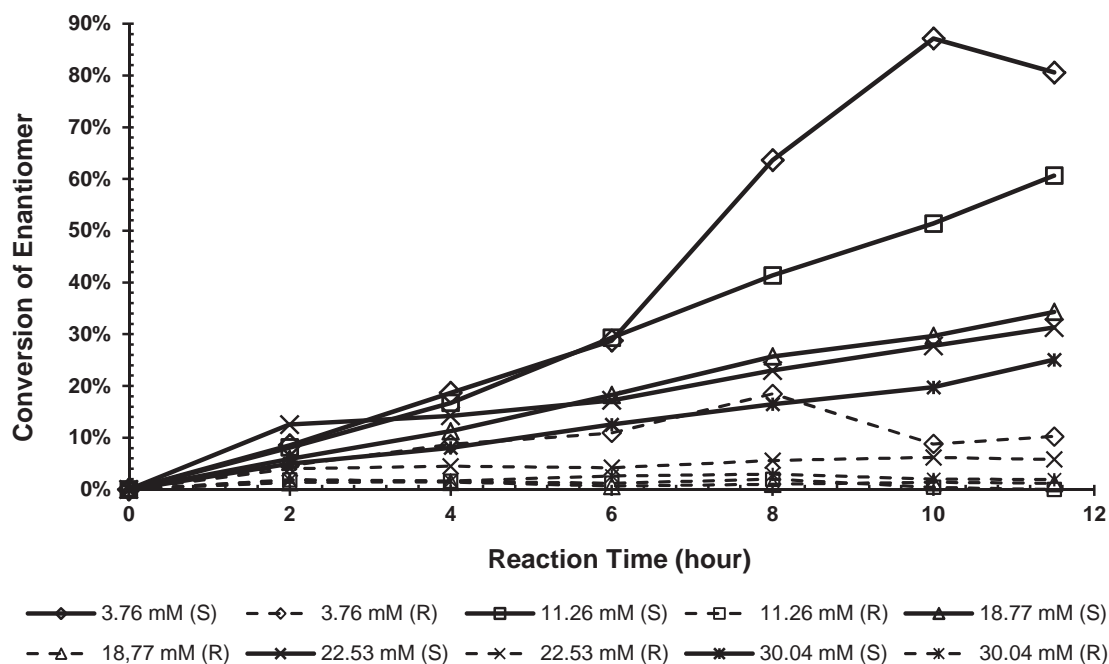


Figure 1 Conversion of both enantiomers at various atenolol concentrations (dashes: (*R*)-atenolol; line in bold: (*S*)-atenolol).

installed on a Shimadzu LC-20A Prominence Ultra Fast Liquid Chromatograph (UFLC). The mobile phase consisted of hexane–ethanol–diethyl amine (75%:25%:0.1% v/v) and was flowed at 0.5 mL/min. A UV/Vis detector was set at the wavelength of 276 nm. The UFLC was operated at the normal phase at 35°C. 2 μ L samples were injected directly without pretreatment. Under these conditions, the (*R*)-atenolol was detected at minute 14.1, whereas the (*S*)-atenolol was observed at minute 16.7.

RESULTS AND DISCUSSION

Conversion of the (*S*)- and (*R*)-atenolol during the initial reaction rate observation at various substrate concentrations is shown in Figs. 1 and 2. The enzyme preferred the (*S*)-enantiomer. Although both enantiomers were changed during the reaction, lower conversions of the (*R*)-atenolol were obtained. In general, 2.69–87.14% of the (*S*)-atenolol and 0–18.47% of the (*R*)-atenolol were converted. The conversions of both enantiomers were high at low substrate concentrations. The highest conversion of the (*S*)-atenolol was obtained at the lowest racemic atenolol concentration (3.76 mM). At this condition, around 87% of the enantiomer was converted. However, the conversion of this enantiomer decreased sharply at the highest substrate concentra-

tion. Under the racemic atenolol concentrations of 11.26–30.04 mM, less than 60% of the (*S*)-atenolol was changed, but the conversions increased steadily at the concentration range. In contrast, only as high as 18.50% of the (*R*)-atenolol reacted with vinyl acetate, which was obtained at the lowest racemic atenolol concentration. Reduction of conversion of the (*R*)-atenolol was observed when the racemic atenolol concentration was increased.

Several factors could cause the decrease of conversion when the racemic atenolol concentration was increased. At low substrate concentrations, as the enzyme activity was constant throughout the trials, many enzyme active sites were available for the substrates. But, at high racemic atenolol concentrations, many acetyl–enzyme complexes were formed and many vinyl acetate molecules still existed in the solution as constant enzyme quantity was used. Hence, the reaction environment was enriched with the (*R*)- and (*S*)-atenolol and vinyl acetate as constant reaction volume was applied. Romero et al. [23] described that properties of medium (e.g., polarity) were modified when alcohol and acetic anhydride concentrations were increased leading to the reaction that may be shifted to the polarest substrate(s), and the free amount of substrates in the medium caused enzyme deactivation. Another possible factor is that the amount of enzyme became the limiting substance at higher substrate concentration [24]. The same results were observed during

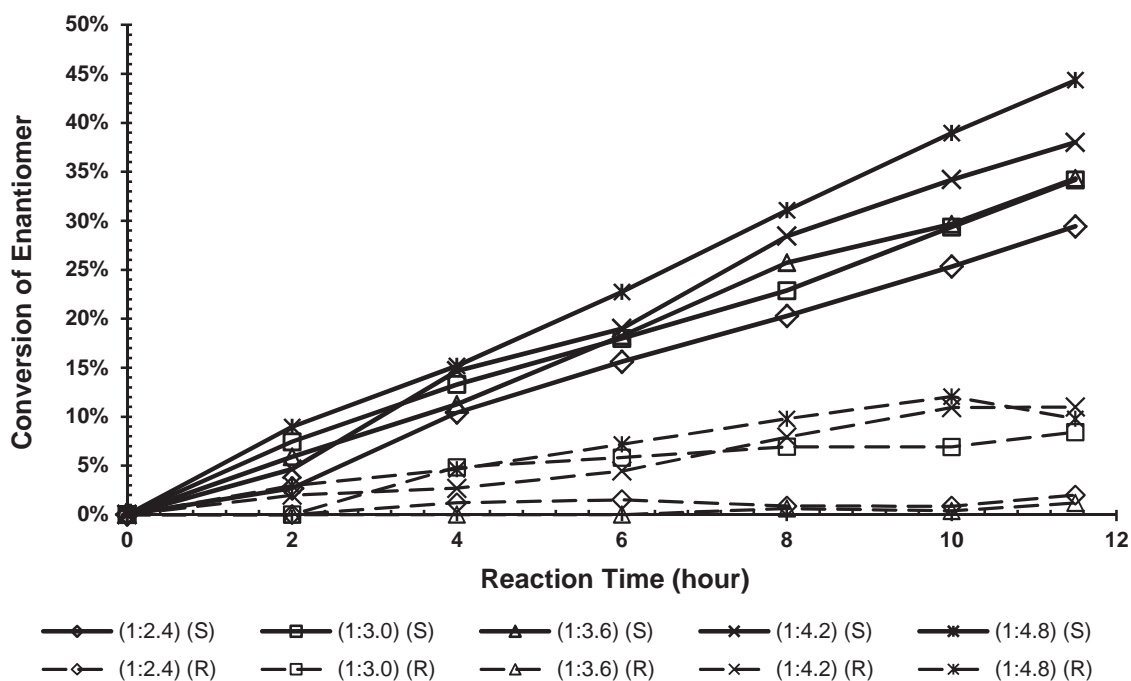


Figure 2 Conversions of enantiomers at different vinyl acetate supply (dashes: (*R*)-atenolol; line in bold: (*S*)-atenolol).

racemic propranolol resolution using *Candida antarctica* lipase B (CALB) [18]; however, resolution of the racemic atenolol using CALB showed increases of conversion when the racemate concentration was changed from 3.30 to 16.60 mM [25].

Since the reaction involves two substrates, the compounds ratio in the reaction must be optimized to give high conversion and to minimize the reactants cost [23]. When the enzymatic reaction was conducted under various vinyl acetate concentrations (the substrates' ratios were set from 1:2.4 to 1:4.8 as described in Fig. 2), conversions of the (*S*)-atenolol increased steadily, which were higher than the (*R*)-atenolol that showed little increases. High concentration of vinyl acetate tended to result in high conversion of both enantiomers. The highest conversion of the (*S*)-atenolol was found at the highest vinyl acetate concentration that was the same as the (*R*)-atenolol. The conversion of 11% was obtained on the (*R*)-atenolol at the highest vinyl acetate concentration. The observed ratio followed the previous results such as Damle et al. [17] used the molar ratio of 1–1.2 to change the (*R*)-atenolol to ester using vinyl acetate or succinic anhydride and lipase PS-D to give 40–42% overall yield. Later, Barbosa et al. [25] used a ratio of vinyl acetate of 2–10 to convert the (*R*)-atenolol, which obtained the conversions of 55–75% where the substrate molar ratio of 2 produced the best result. Some acetylation-based enzymatic processes used 1–5 molar ratios [26–30].

Comparison of the reaction rate of both atenolol enantiomers is shown in Fig. 3. The transesterification reaction rate for the (*S*)-atenolol is higher than the (*R*)-atenolol. The reaction rate of the (*S*)-atenolol was 4.73–126.32 times higher than that of the (*R*)-atenolol. The enantiomeric ratio (*E* value) of the enzyme in the kinetic resolution can be calculated from the ratio of the two reaction rates (the transesterification reaction rate of the (*S*)-atenolol over the (*R*)-atenolol), which in this case the *E* values were about 5–62. Since the (*R*)-atenolol was found to be less reactive in the kinetic resolution, assumption of one substrate and one product was applied in the enzymatic reaction.

Kinetics without Accounting Inhibition

Kinetics of the racemic atenolol transesterification was first developed without inclusion of the inhibition process to justify that the enzymatic reaction was operated at minimum inhibition effect(s). The kinetics was estimated by using Michaelis–Menten and Lineweaver–Burk plots on the enzymatic reaction mechanisms. Theoretically, in the lipase-catalyzed transesterification, it has been established that the lipase first forms an acetyl–enzyme complex with the acetyl donor, which rules out the random mechanism of the enzymatic reaction [31–33]. Thus, in estimating the kinetic parameters using the software, vinyl acetate was entered first. The schematic diagrams of available enzymatic

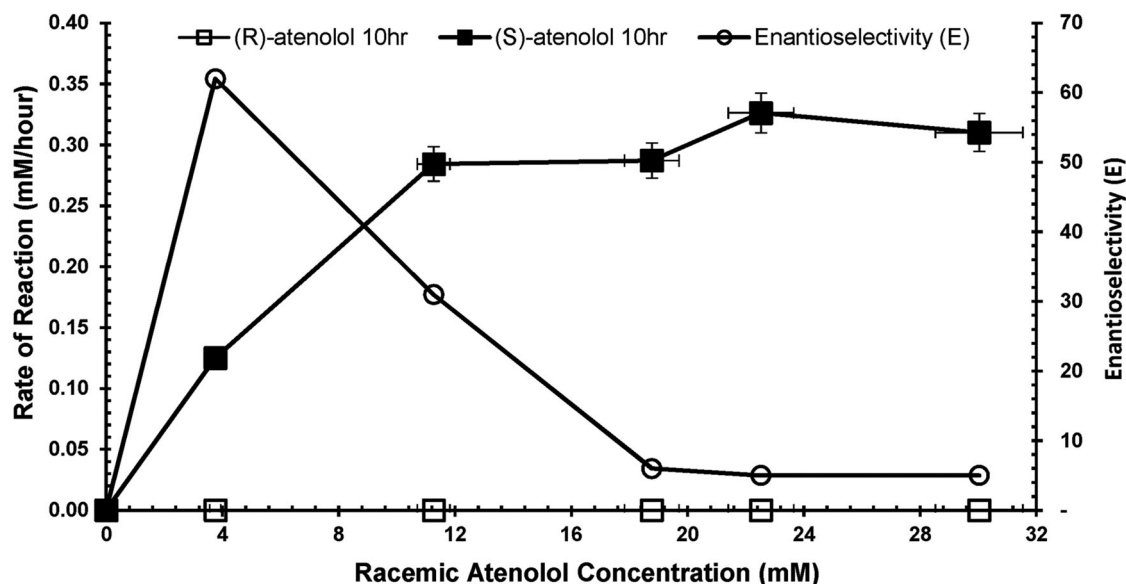
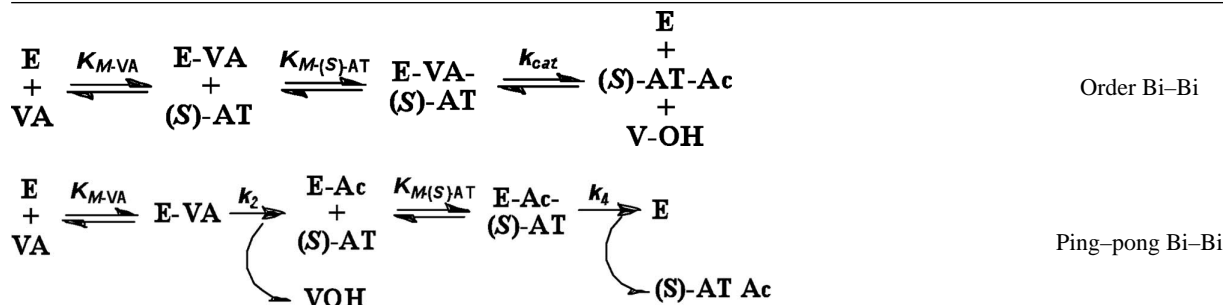


Figure 3 Rate of reaction of the (*S*)- and (*R*)-atenolol transesterification as a function of racemic atenolol concentration after 10 h reaction.

Table I The Predicted Enzymatic Reaction Mechanisms without Inhibition



E: enzyme; VA: vinyl acetate; (S)-AT: (*S*)-atenolol; (S)-AT-Ac: (*S*)-atenolol acetate; Ac: acetate; VOH: vinyl alcohol.

reaction mechanisms without any inhibition process are given in Table I. The Michaelis–Menten graphs for these mechanisms are shown in Fig. 4. The graph indicates that a first-order reaction occurred. The ordered Bi–Bi mechanism produces a better graphical representation of the reaction rates as parallel lines were formed within the trial concentrations. The ping–pong Bi–Bi mechanism showed almost the same rate of reaction at the (*S*)-atenolol concentration of less than 2 (two) mM.

Results of the calculation for these mechanisms produce the same coefficient of determination (R^2) (Table II). Although the R^2 are not high (the closer the value of the R^2 to 1 (one), the better the model predicts the dependent variables), the results are considered acceptable for kinetic resolution of a racemic compound

(R^2 for good correlations are 70–100% [34–36]). None article on the racemic compound kinetic resolution was found mentioning the R^2 values on a selected mechanism; hence a comparison cannot be made. The Akaike information criterion correction (AICc) values on both mechanisms are excellent as low results are obtained. The values of the AICc for the ordered-sequential Bi–Bi and ping–pong Bi–Bi mechanism are around –170. Low AICc values correspond to better fits the model to the data [37]. Values of sum of squares for both mechanisms are <8%, indicating smaller random error component(s) on the models. The probability values (P values) are good where they almost approach the significance of 5% (the suggested P value in Sigma–Plot calculation [38]). Therefore, these mechanisms' models are acceptable.

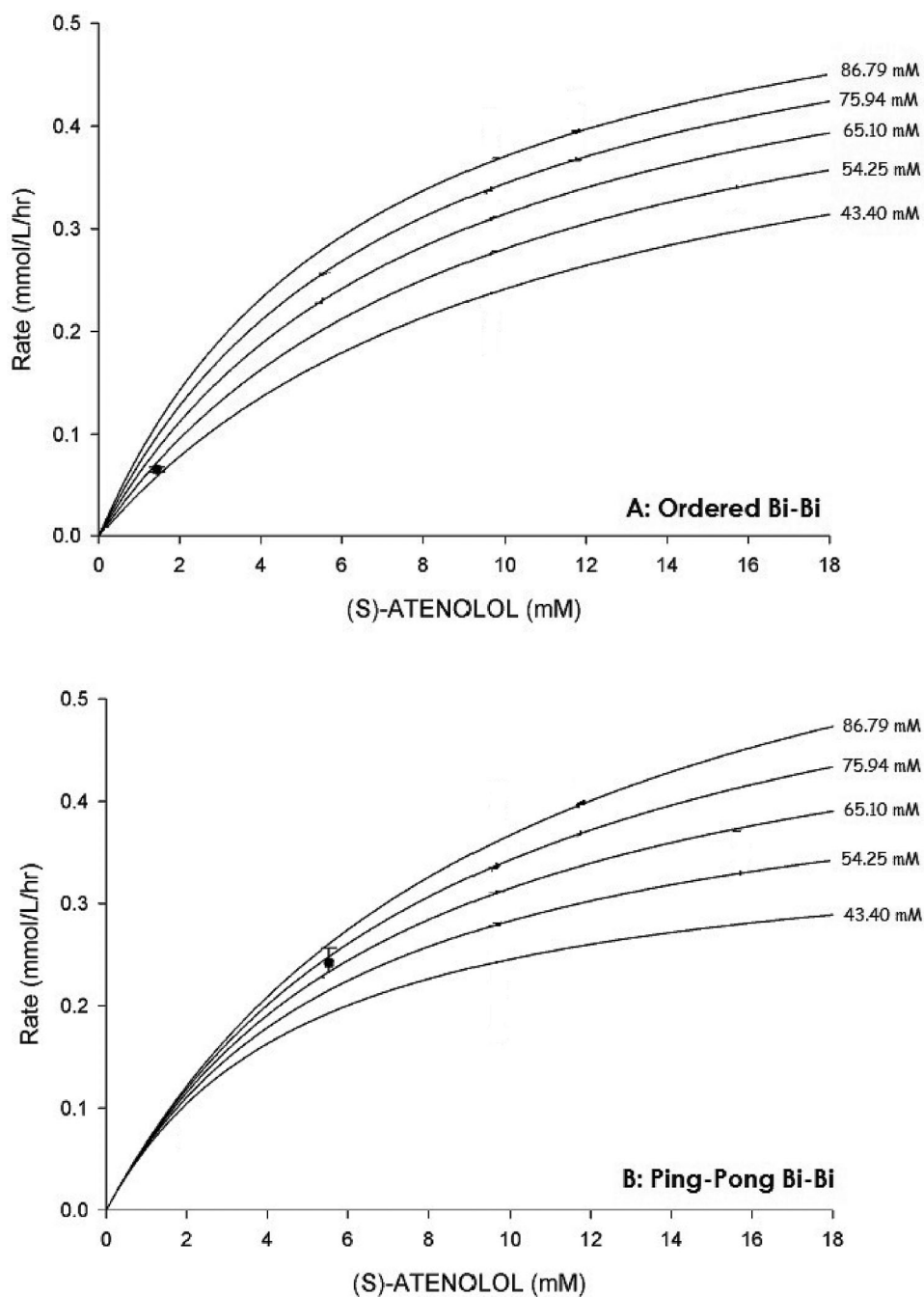


Figure 4 Michaelis–Menten plots on various vinyl acetate concentrations as a function of (*S*)-atenolol concentration.

By comparing the V_{\max} value, the ping–pong Bi–Bi mechanism gave higher result (4492.99 mmol/L/h) than the ordered-sequential Bi–Bi mechanism (0.80 mmol/L/h). The V_{\max} for the ping–pong Bi–Bi mechanism exceeds the experimental reaction rates. As can be seen from Fig. 4, the reaction rates of less than 1 (one) mmol/L/h were used to develop the Michaelis–

Menten graphs within the applied concentrations of both substrates. Hence, the ordered-sequential Bi–Bi mechanism was acceptable as its V_{\max} does not differ highly with the experimental reaction rates. Values of the Michaelis constants for the ordered-sequential Bi–Bi mechanism were lower than the Michaelis constants for the ping–pong Bi–Bi. Low Michaelis constants are

Table II Comparison of the Available Mechanisms' Results

Item	Ordered-Sequential		Ping-Pong Nonsequential	
	Value	SEE	Value	SEE
V_{\max} (mM/h)	0.80	0.39	4,492.99	1.46×10^7
K_a (mM)	29.22	46.65	61,892.92	2.01×10^8
K_b (mM)	25.42	48.12	5.269×10^5	1.71×10^9
AICc	-170.97		-170.86	
R^2	75.0%		74.9%	
Sum of squares	0.073		0.073	
Residual SD	0.053		0.052	
P value	0.064		0.064	

mM: millimolar; h: hour; AICc: Akaike Information Criterion correction; R^2 : coefficient of determination; SEE: standard error of estimation; SD: standard deviation, K_a : Michaelis constant for vinyl acetate; K_b : Michaelis constant (*S*)-atenolol.

expected to give high enzymatic reaction rates since these constants are a denominator in mathematical formulas as shown in the previous equations. As the standard error of estimation for the ping-pong Bi-Bi mechanism is extremely high; therefore, the ordered-sequential Bi-Bi mechanism is the most appropriate kinetic model for the enzymatic transesterification of the racemic atenolol using vinyl acetate.

Equation (1) describes the final form of the racemic atenolol transesterification enzyme kinetics based on the ordered-sequential Bi-Bi mechanism for a two substrates reaction without the compound(s) inhibition:

$$v = \frac{V_{\max} [\mathbf{A}] [\mathbf{B}]}{K_a K_b + K_b [\mathbf{A}] + [\mathbf{A}] [\mathbf{B}]} = \frac{(0.80) ([\mathbf{VA}] ([\mathbf{S}] - \mathbf{AT}))}{742.77 + 25.42 ([\mathbf{VA}]) + ([\mathbf{VA}]) ([\mathbf{S}] - \mathbf{AT})} \quad (1)$$

Enzyme Kinetics Accounting Inhibition

The presence of the compound(s) that inhibits the enzymatic transesterification reaction is confirmed by Lineweaver-Burk and Eadie-Hofstee plot. The inhibitions caused by the substrates were clearly observed. However, the inhibition developed by product(s) were ignored as the (*S*)-atenolol acetate is not available commercially; hence, it cannot be investigated separately to know its effect(s). Furthermore, inhibition caused by (*R*)-atenolol was also unaccounted.

Identification of the inhibition type through the Lineweaver-Burk plot for the ordered-sequential Bi-Bi mechanism is shown in Fig. 5. By comparing both graphs with literature sources [39,40], it could be pre-

dicted that the inhibition caused by the (*S*)-atenolol is competitive type, whereas vinyl acetate shows a mixed inhibition process. The inhibition caused by vinyl acetate, when its concentrations were increased, was low as the value of the V_{\max} decreased slightly. But, (*S*)-atenolol produced low effect at the concentration of less than 9.70 mM as small differences were observed on Michaelis constant values. At higher (*S*)-atenolol concentrations, the inhibition effects increased rapidly. Based on the inhibition process, new reaction mechanism and equation for predicting kinetic constants, which include the inhibition, must be established.

Competitive Inhibition by (*S*)-Atenolol (**A**)

Table III shows the new enzymatic ordered-sequential Bi-Bi mechanism for the competitive inhibition by the (*S*)-atenolol. The rate of reaction is defined as

$$\frac{V_{\max}}{v} = \frac{K_a K_b}{[\mathbf{VA}] [(S) - \mathbf{AT}]} + \frac{K_b}{[(S) - \mathbf{AT}]} + 1 + \frac{K_a K_b}{K_I [\mathbf{VA}]} \quad (2)$$

The new forms of Eq. (2) under constant (*S*)-atenolol concentration and various vinyl acetate concentrations and vice versa are shown in Table IV. To obtain the inhibition constant, these equations are linearized ($y = 1/v$, $x = 1/[\text{substrate}]$). Linear regression of the reaction rates versus (*S*)-atenolol concentration (Fig. 6) gives K_I in the intercept portion (Table IV). In the same way, plot of the reaction rates versus vinyl

acetate concentration results the K_I in the slope portion. As K_I is positive, the competitive inhibition by (*S*)-atenolol indeed occurs.

Mixed Inhibition by Vinyl Acetate (**B**)

The second inhibition type observed in the reaction is mixed inhibition by vinyl acetate. It is characterized by attachment of an inhibitor on two positions: to free enzyme (**E**) on sites other than the active sites to form the enzyme-inhibitor complex (**EI**) and to enzyme-substrate complex (**ES**) to give enzyme-substrate-inhibitor complex (**ESI**) [41]. There are three possibilities for vinyl acetate to attach to the enzyme to inhibit the reaction as described in the mechanism shown in

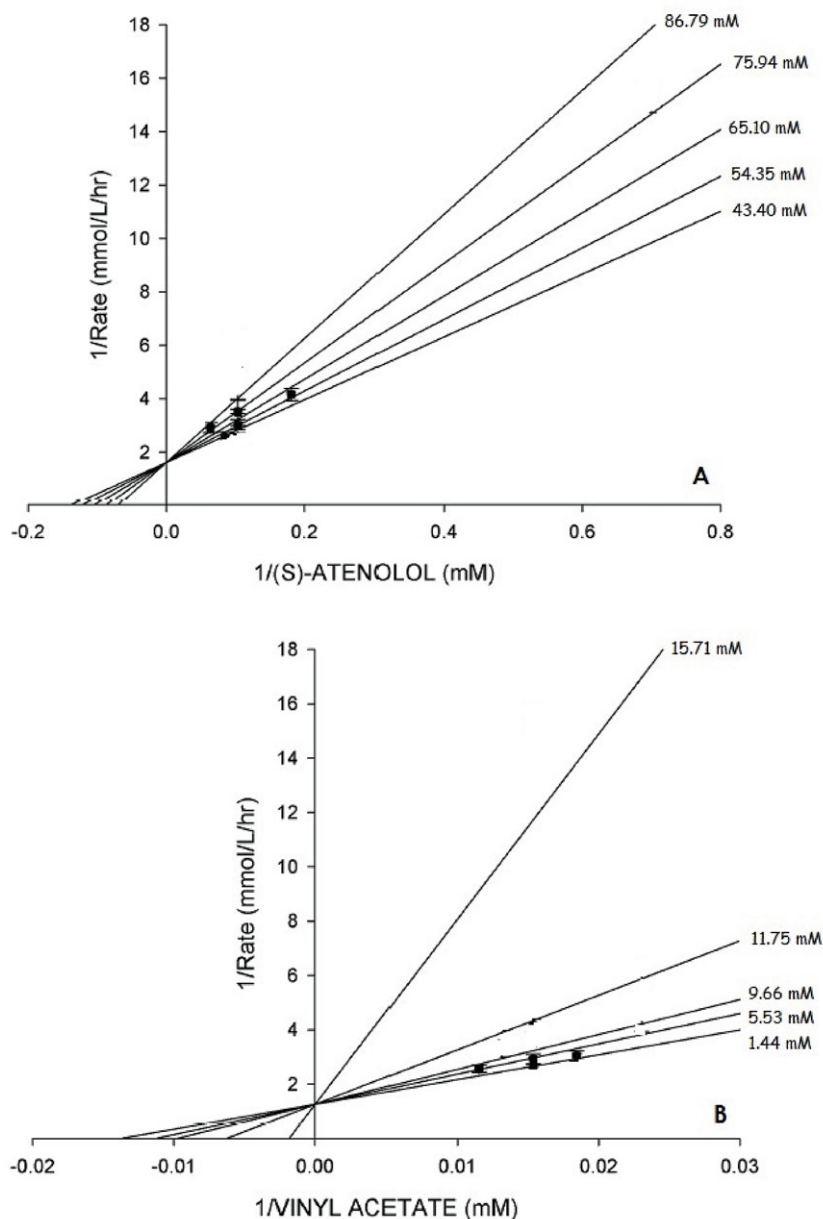


Figure 5 Lineweaver–Burk plots of the ordered-sequential Bi–Bi mechanism: (A) various (S)-atenolol concentrations and (B) various vinyl acetate concentration.

Table III. The rate of reaction is given as below.

$$\frac{v}{V_{\max}} = \frac{1}{\frac{K_a K_b}{[VA][(S)-AT]} + \frac{K_b}{[(S)-AT]} + 1 + \frac{K_a K_b}{K_{I1}[(S)-AT]} + \frac{K_b [VA]}{K_{I2}[(S)-AT]} + \frac{[VA]}{K_{I3}}} \quad (3)$$

The forms of Eq. (3) at constant (S)-atenolol concentration or vinyl acetate concentration are given in Table IV. Linear regression of the Eq. (3) against (S)-atenolol concentration ($y = 1/v$, $x = 1/[(S)\text{-atenolol}]$;

Fig. 6) produces K_{I3} in the intercept portion, whereas other constants described in the slope part cannot

be solved. Plotting Eq. (3) against the vinyl acetate concentration ($y = a^*x + b/x + c$, $y = 1/v$, $x = [\text{vinyl acetate}]$); Fig. 7) gives a nonlinear equation that is solved using Polymath to yield K_{I2} and K_{I1} (Table IV). K_{I2}

Table III Enzymatic Reaction Mechanisms for the Inhibition Processes

Inhibition	Code	Mechanism
Competitive inhibition by (S)-atenolol	A	$\begin{array}{c} \text{E} + \text{VA} \xrightleftharpoons{K_a} \text{E.VA} + (\text{S})\text{-AT} \xrightleftharpoons{K_b} \text{E.VA.}(\text{S})\text{-AT} \xrightarrow{k_{cat}} \text{E} + \text{P} + \text{Q} \\ + \\ (\text{S})\text{-AT} \\ \downarrow \uparrow K_I \\ \text{E.}(\text{S})\text{-AT} \end{array}$
Mixed inhibition by vinyl acetate	B	$\begin{array}{c} \text{E} + \text{VA} \xrightleftharpoons{K_a} \text{E.VA} + (\text{S})\text{-AT} \xrightleftharpoons{K_b} \text{E.VA.}(\text{S})\text{-AT} \xrightarrow{k_{cat}} \text{E} + \text{P} + \text{Q} \\ + \quad \quad \quad + \quad \quad \quad + \\ \text{VA} \quad \quad \quad \text{VA} \quad \quad \quad \text{VA} \\ \downarrow \uparrow K_{I1} \quad \quad \quad \downarrow \uparrow K_{I2} \quad \quad \quad \downarrow \uparrow K_{I3} \\ \text{E.VA}^* + \text{VA} \xrightleftharpoons{K_a'} \text{E.VA}^*.\text{VA} + (\text{S})\text{-AT} \xrightleftharpoons{K_b'} \text{E.VA}^*.\text{VA.}(\text{S})\text{-AT} \end{array}$
Both substrates inhibition	C	$\begin{array}{c} \text{E} + \text{VA} \xrightleftharpoons{K_a} \text{E.VA} + (\text{S})\text{-AT} \xrightleftharpoons{K_b} \text{E.VA.}(\text{S})\text{-AT} \xrightarrow{k_{cat}} \text{E} + \text{P} + \text{Q} \\ + \quad \quad \quad + \quad \quad \quad + \\ (\text{S})\text{-AT} \quad \quad \quad \text{VA} \quad \quad \quad \text{VA} \\ \downarrow \uparrow K_{I1} \quad \quad \quad \downarrow \uparrow K_{I2} \quad \quad \quad \downarrow \uparrow K_{I3} \\ \text{E.}(\text{S})\text{-AT} \quad \text{E.VA.VA}^* + (\text{S})\text{-AT} \xrightleftharpoons{K_b'} \text{E.VA.VA}^*.\text{(S)-AT} \end{array}$
	D	$\begin{array}{c} \text{E} + \text{VA} \xrightleftharpoons{K_a} \text{E.VA} + (\text{S})\text{-AT} \xrightleftharpoons{K_b} \text{E.VA.}(\text{S})\text{-AT} \xrightarrow{k_{cat}} \text{E} + \text{P} + \text{Q} \\ + \quad \quad \quad + \quad \quad \quad + \\ (\text{S})\text{-AT} \quad \quad \quad \text{VA} \\ \downarrow \uparrow K_I \quad \quad \quad \downarrow \uparrow K_{I3} \\ \text{E.}(\text{S})\text{-AT} \quad \quad \quad \text{E.VA.VA}^*.\text{(S)-AT} \end{array}$

E: enzyme, VA: vinyl acetate, (S)-AT: (S)-atenolol, K_a : Michaelis constant for vinyl acetate, K_b : Michaelis constant for (S)-atenolol, K_I : inhibition constant, P: (S)-atenolol acetate, Q: vinyl alcohol, K_{I1} : inhibition constant 01, K_{I2} : inhibition constant 02, K_{I3} : inhibition constant 03, K_a' : modified Michaelis constant for vinyl acetate, K_b' : modified Michaelis constant for (S)-atenolol. "*" indicates nonenzyme' active sites attachment.

and K_{I3} are positive meaning the inhibition proceeds within the pathway.

Enzyme Kinetics with Both Substrates Inhibitions

There are some mechanisms that can be used to develop the simultaneous inhibition by both substrates (Table III, C and D). The first alternative (C) uses the previous mixed mechanism, but free enzyme (E) associates with (S)-atenolol to form the dead-end enzyme-(S)-atenolol complex. Normalization of the reaction rate gives

At various (S)-atenolol or vinyl acetate concentrations, Eq. (4) can be simplified into the equations shown in Table IV. Under various (S)-atenolol concentrations, linear regression of Eq. (4) produces K_{I2} in the slope part. Variations of the vinyl acetate concentrations give a nonlinear equation $y = a^*x + b/x + c$ ($y = 1/v$, $x = [\text{vinyl acetate}]$; Fig. 7) then solved by Polymath to give K_{I1} and K_{I3} . Two positive values are found (K_{I1} and K_{I3}) confirming inhibitions indeed occur following the predicted mechanism.

Another inhibition mechanism developed to predict both substrates inhibition is illustrated in pathway D (Table III). The reaction rate is defined as

$$\frac{v}{V_{\max}} = \frac{1}{\frac{K_a K_b}{[\text{VA}][(\text{S})\text{-AT}] + \frac{K_b}{[(\text{S})\text{-AT}] + 1 + \frac{K_a K_b}{K_{I1}[\text{VA}] + \frac{K_b[\text{VA}]}{K_{I2}[(\text{S})\text{-AT}] + \frac{[\text{VA}]}{K_{I3}}}} \quad (4)$$

Table IV The Inhibition Kinetics Equations and the Constants

Type	Reaction Rate Equation			Constant (mM)
	Constant [(S)-Atenolol], Various [Vinyl Acetate]	Various [(S)-Atenolol], Constant [Vinyl Acetate]		
A	$\frac{V_{max}}{v} = \left\{ \frac{K_a K_b}{[(S) - AT]} + \frac{K_a K_b}{K_I} \right\} \frac{1}{[VA]} + \left\{ \frac{K_b}{[(S) - AT]} + 1 \right\}$	$\frac{V_{max}}{v} = \left\{ \frac{K_a K_b}{[VA]} + K_b \right\} \frac{1}{[(S) - AT]} + \left\{ 1 + \frac{K_a K_b}{K_I [VA]} \right\}$	$K_I = 27.74$	
B	$\frac{V_{max}}{v} = \left\{ \left\{ \frac{K_b}{K_{I2}[(S) - AT]} + \frac{1}{K_{I3}} \right\} [VA] + \left(\frac{K_a K_b}{[(S) - AT]} \right) \frac{1}{[VA]} \right. \\ \left. + \left(\frac{K_a K_b}{[(S)AT]K_{I1}} + \frac{K_b}{[(S) - AT]} + 1 \right) \right\}$	$\frac{V_{max}}{v} = \left\{ \frac{K_a K_b}{[VA]} + K_b + \frac{K_a K_b}{K_{I1}} + \frac{K_b [VA]}{K_{I2}} \right\} \frac{1}{[(S) - AT]} + \left\{ 1 + \frac{[VA]}{K_{I3}} \right\}$	$K_{I1} = 0$ $K_{I2} = 1736.13$ $K_{I3} = 160.62$	
C	$\frac{V_{max}}{v} = \left\{ \frac{K_b}{[(S) - AT]K_{I2}} + \frac{1}{K_{I3}} \right\} [VA] + \left\{ \frac{K_a K_b}{[(S) - AT]} + \frac{K_a K_b}{K_{I1}} \right\} \frac{1}{[VA]} \\ + \left\{ \frac{K_b}{[(S) - AT]} + 1 \right\}$	$\frac{V_{max}}{v} = \left\{ \frac{K_a K_b}{[VA]} + K_b + \frac{K_b [VA]}{K_{I2}} \right\} \frac{1}{[(S) - AT]} + \left\{ 1 + \frac{K_a K_b}{[VA]K_{I1}} + \frac{[VA]}{K_{I3}} \right\}$	$K_{I1} = 13.34$	
D	$\frac{V_{max}}{v} = \left\{ \frac{1}{K_{I3}} \right\} [VA] + \left\{ \frac{K_a K_b}{[(S) - AT]} + \frac{K_a K_b}{K_{I1}} \right\} \frac{1}{[VA]} + \left\{ \frac{K_b}{[(S) - AT]} + 1 \right\}$	$\frac{V_{max}}{v} = \left\{ \frac{K_a K_b}{[VA]} + K_b \right\} \frac{1}{[(S) - AT]} + \left\{ \frac{K_a K_b}{[VA]K_{I1}} + \frac{[VA]}{K_{I3}} + 1 \right\}$	$K_{I2} = 0$ $K_{I3} = 20.48$ $K_{I1} = 13.35$ $K_{I3} = 129.12$	

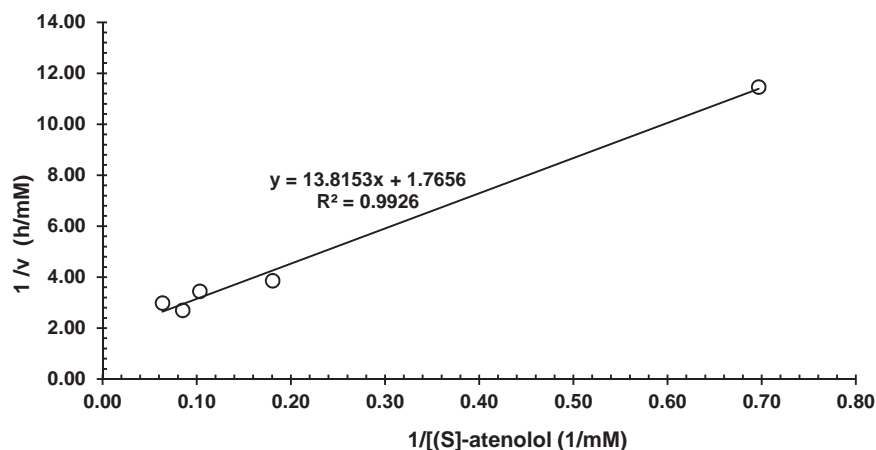


Figure 6 Linear regression plot of (S)-atenolol competitive inhibition.

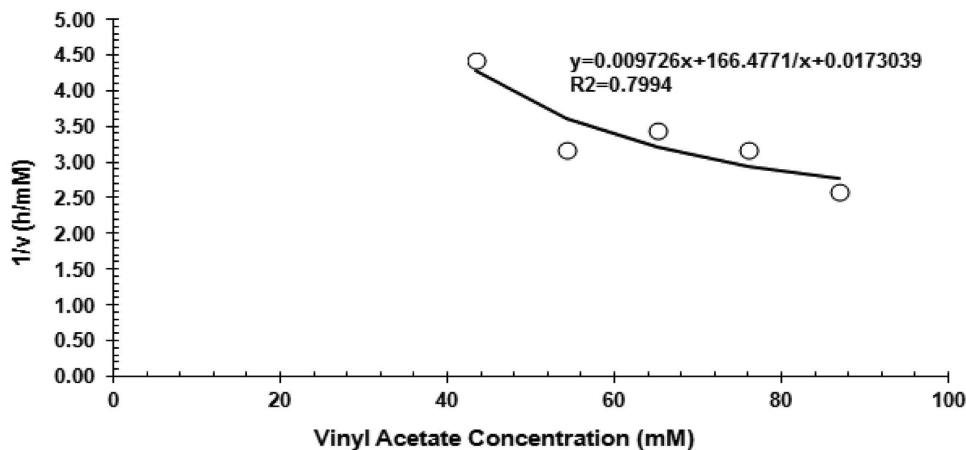


Figure 7 Nonlinear regression plot of vinyl acetate mixed inhibition.

$$\frac{v}{V_{\max}} = \frac{1}{\frac{K_a K_b}{[VA][(S)-AT]} + \frac{K_b}{[(S)-AT]} + 1 + \frac{K_a K_b}{K_{I1}[VA]} + \frac{[VA]}{K_{I3}}} \quad (5)$$

When (S)-atenolol or vinyl acetate concentration is varied, Eq. (5) can be derived to find the inhibition constants as shown in Table IV. At constant (S)-

The form of the final equation for the racemic atenolol transesterification enzyme kinetics based on the sequential ordered Bi-Bi mechanism for a two-substrate reaction with mixed inhibition by the substrates is as follows:

$$\frac{v}{V_{\max}} = \frac{[A][B]}{K_a K_b + K_b [A] + [A][B] + \frac{K_a K_b [B]}{K_{I1}} + \frac{[A][A][B]}{K_{I3}}} \quad (6)$$

$$= \frac{(0.80)(VA)((S) - AT)}{742.77 + (25.42)([VA]) + ([VA])((S) - AT) + \frac{742.77((S)-AT)}{13.35} + \frac{[VA][VA][(S)-AT]}{129.12}} \quad (7)$$

atenolol concentration, a nonlinear equation is formed ($y = a^*x + b/x + c$; $y = 1/v$, $x = [\text{vinyl acetate}]$; Fig. 7) then solved with Polymath nonlinear regression to give K_{I1} and K_{I3} . As both inhibition constants are positive, the possible inhibition mechanism is established.

CONCLUSION

Analysis of the racemic atenolol transesterification enzyme kinetics using Michaelis-Menten and

Lineweaver–Burk plot resulted first-order reaction and ordered-sequential Bi-Bi mechanism with R^2 : ~75%. V_{\max} , K_M -vinyl acetate, K_M -(*S*)-atenolol are 0.80 mmol/L/h, 29.22 mM, and 25.42 mM. After observing the inhibition phenomena using the Lineweaver–Burk plot, both substrates inhibit the enzymatic reaction where the (*S*)-atenolol and vinyl acetate develop the competitive inhibition and mixed inhibition process, respectively. The inhibition created by the (*S*)-atenolol was low at low (*S*)-atenolol concentrations, but the inhibition effects increased rapidly at high (*S*)-atenolol concentrations; however, vinyl acetate shows a low inhibition effect throughout the trial concentrations. The inhibition constants for the (*S*)-atenolol is 13.35 mM whereas for the vinyl acetate is 129.12 mM.

Financial supports from Universiti Sains Malaysia (PRGS: 1001/PJKIMIA/8044030), MOSTI (Science Fund: 305/227/PJKIMIA/6013337), MTDC (304/PJKIMIA/6053010) for the research were deeply acknowledged. Joni Agustian thanks to the MTCP scholarship from MOHE, USM Graduate Assistant Scheme, and USM Graduate Research Assistant Scheme for assisting his study.

BIBLIOGRAPHY

- Hara, T. *Innovations in the Pharmaceuticals Industry: The Process of Drug Discovery and Development*; Edward Elgar : Cheltenham, UK, 2003.
- Sneader, W. *Drug Discovery: A History*; Wiley: Chichester, UK, 2005.
- Westfall, T. C.; Westfall, D. P. In *Goodman and Gilman's The Pharmacological Basis of Therapeutics*; 11th ed.; Brunton, L. L.; Lazo, J. S.; Parker, K. L., Eds. McGraw-Hill: New York, 2006, pp. 237–247.
- Stoschitzky, K.; Egginger, G.; Zernig, G.; Klein, W.; Lindner, W. *Chirality* 1993, 5, 15–19.
- Stoschitzky, K.; Kahr, S.; Donnerer, J.; Schumacher, M.; Luha, O.; Maier, R.; Klein, W.; Lindner, W. *Clin Pharmacol Ther* 1995a, 57, 543–551.
- Stoschitzky, K.; Lindner, W.; Kiowski, W. *J Cardiovasc Pharmacol* 1995b, 25, 268–272.
- Kumar, A.; Vyas, K. D.; Singh, D.; Mahale, G. D.; Nellithanath, T. B.; Nandavadekar, S.; Jadhav, B. G.; Saxena, A. K. N. K.; Dharji, M. K.; Bhattacharya, A.; Lakhera, A. *WIPO Pat. WO 2006/046252 A2*, 2006.
- Bose, D. S.; Narsaiah, A. V. *Bioorg Med Chem* 2005, 13, 627–630.
- Kawthekar, R. B.; Bi, W. T.; Kim, G. J. *Appl Organometal Chem* 2008, 22, 583–591.
- Kawthekar, R. B.; Kim, G. J. *Helv Chim Acta* 2008, 91, 317–332.
- R. B. Kawthekar, W. T. Bi, G. J. Kim, *Bull Korean Chem Soc* 2008, 29, 313.
- Dwivedee, B. P.; Ghosh, S.; Bhaumik, J.; Banotha, L.; Banerjee, U. C. *RSC Adv* 2015, 5, 15850–15860.
- Kitaori, K.; Takehira, Y.; Furukawa, Y.; Yoshimoto, H.; Otera, J. *Chem Pharm Bull* 1997, 45(2), 412–414.
- Takehira, Y.; Saragai, N.; Kitaori, K. *US Pat. US005, 130,482A*, 1992.
- Takehira, Y.; Saragai, N.; Kitaori, K. *US Pat. US005, 223,646A*, 1993.
- Damle, S. V.; Patil, P. N.; Salunkh, M. S. *Bioorg Med Chem* 2000, 8, 2067–2070.
- Damle, S. V.; Patil, P. N.; Salunkhe, M. M. *Synth Commun* 1999, 29(22):3855–3862.
- Barbosa, O.; Ariza, C.; Ortiz, C.; Torres, R. *New Biotechnol* 2010, 27(6), 844–850.
- Bhushan, R.; Aora, M.; *Biomed Chromatogr* 2003, 17, 226–230.
- Bhushan, R.; Tanwar, S.; *Biomed Chromatogr* 2008, 22, 1028–1034.
- Zhang, H.; Shao, H.; Youmei, A.; Zhang, A. *Chromatographia* 2008, 68, 653.
- Duan, G.; Ching, C. B.; Lim, E.; Ang, C. H. *Biotechnol Lett* 1997, 19(11), 1051–1055.
- Romero, M. D.; Calvo, L.; Alba, C.; Daneshfar, A. *J Biotechnol* 2007, 127, 269–277.
- Ong, A. L.; Kamaruddin, A. H.; Bhatia, S.; Long, W. S.; Lim, S. T.; Kumari, R. *Enzyme Microbiol Technol* 2006, 39, 924–929.
- Barbosa, O.; Ortiz, C.; Torres, R.; Fernandez-Lafuente, R. *J Molec Catal B* 2011, 71, 124–132.
- Ghanem, A.; Schurig, V. *Tetrahedron: Asymmetry* 2003, 14, 57–62.
- Pchelka, B. K.; Loupy, A.; Plenkiewicz, J.; Petit, A.; Blanco, L. *Tetrahedron: Asymmetry* 2001, 12, 2109–2119.
- Pchelka, B. K.; Loupy, A.; Plenkiewicz, J.; Blanco, L. *Tetrahedron: Asymmetry* 2000, 11, 2719–2732.
- Kawasaki, M.; Goto, M.; Kawabata, S.; Kodama, T.; Kometani, T. *Tetrahedron Lett* 1999, 40, 5223–5226.
- Kawasaki, M.; Goto, M.; Kawabata, S.; Kodama, T.; Kometani, T. *Tetrahedron: Asymmetry* 2000, 12, 585–596.
- Faber, K.; Riva, S. *Synthesis* 1992, 24, 895–910.
- Yadav, G. D.; Sivakumar, P. *Biochem Eng J* 2004, 19, 101–107.
- Sontakke, J. B.; Yadav, G. D. *Ind Eng Chem Res* 2011, 50, 12975–12983.
- Morningstar, R-squared; available from http://www.morningstar.com/InvGlossary/r_squared.definition.what.is.aspx, accessed on December 9, 2015.
- Ron, P. What is a good R-squared value or is the fit good for a trend line?; available at <http://www.criticaltosuccess.com/>; accessed December 9, 2015.

36. Udovicic, M.; Baždarić, K.; Bilić-Zulle, L. *Biochem Med* 2007, 17(1), 10–15.
37. Mitchell, D. Available at <https://systatsoftware.com/> accessed on July 31, 2013.
38. Systat Software Inc. SigmaPlot® 11: Analyse and graph your data with unparalleled ease and precision. Part 2–Statistics; Systat Software; San Jose, CA, 2008.
39. Sharma, R. In *Enzyme Inhibition and Bioapplication*; Sharma, R., Ed.; Intech Publisher: Rijeka, Croatia, 2012, pp. 3–36.
40. Bisswanger, H. *Enzyme Kinetics: Principles and Methods*; Wiley-VCH: Weinheim, Germany, 2002.
41. Marangoni, A. G. *Enzyme Kinetics: A Modern Approach*; Wiley : Hoboken, NJ, 2003.